Isotopic signatures of methane emission from oil and natural gas plants in southwestern China

Dingxi Chen[1†], Yi Liu[2†], Zetong Niu[1], Ao Wang[1], Pius Otwil[1], Yuanyuan Huang[1], Zhongcong Sun[1], Xiaobing Pang[3], Liyang Zhan[4], Longfei Yu[1, 5*]

[1]Shenzhen Key Laboratory of Ecological Remediation and Carbon Sequestration, Institute of Environment and Ecology, Tsinghua Shenzhen International Graduate School, Tsinghua University, Shenzhen 518055, China

[2]Safety, Environment and Technology Supervision Research Institute of PetroChina Southwest Oil and Gas Field Company, Chengdu 610041, China

[3]College of Environment, Zhejiang University of Technology, Hangzhou, 310014, China

[4]Key Laboratory of Global Change and Marine-Atmospheric Chemistry, Third Institute of Oceanography, Ministry of Natural Resources, Xiamen, 361005, China

[5]Xinjiang Institute of Ecology and Geography, Chinese Academy of Sciences, Urumqi, 830011, China

[*]Corresponding authors: longfei.yu@sz.tsinghua.edu.cn

[†]These authors contributed equally.

Manuscript Type: Research Article

Abstract

Current evaluation of methane (CH_4) emissions to the atmosphere from global oil and gas (ONG) sector are subject to considerable uncertainty. Particularly for China, few measurements have been conducted, making it difficult to quantify emissions and conduct mitigation measures. Recently, the isotopic composition of CH_4 ($\delta^{13}C$) has been used for evaluating the contributions of fossil fuel sources to global budgets, providing a more effective approach across both regional and global scales. Here, we present a field study of CH_4 mixing ratios and $\delta^{13}C$ based on UAV sampling and ground monitoring across 11 ONG sites located in southwestern China. We found that the values of $\delta^{13}C$-CH_4 provide a solid basis for identifying the CH_4 leakage and characterizing source distributions at the ONG site-levels, despite that the meteorological and site conditions as well as the surrounding environment could exert influence on the signal strengths. With the Keeling plot approach, we determined that the mean $\delta^{13}C$ source isotopic signatures of CH_4 emission from these ONG sites were -25.66 ‰, heavier than previously found for other sites globally. This also indicates that they were mainly thermogenic sources. Finally, by incorporating the updated source isotopic signatures determined for China, we conducted a back-of-envelope assessment to qualitatively infer the global CH_4 emission from the fossil fuel sources. The result suggests an overestimation emission of global CH_4 from the fossil fuel inventory by 2.86 Tg CH_4 yr^{-1}, and an underestimation from the microbial sources. This study highlights the necessity of determining CH_4 isotopes on ONG site-levels, providing indirect but important reference to quantifying CH_4 inventories among global industrial sectors.

1 Introduction

Methane (CH_4) is a major greenhouse gas (GHG) in the atmosphere, with a global warming potential 82.5 times greater than carbon dioxide (CO_2) over a 20-year timeline, and 29.8 times greater over a 100-year period (Intergovernmental Panel on Climate Change, 2021). The mixing ratios of CH_4 in the atmosphere has increased by 150% since the industrial revolution, primarily driven by human activities (Hmiel et al., 2020; Tian et al., 2016; Skeie et al., 2023; Saunois et al., 2024; Nisbet et al., 2025). However, for the past decades, the major paradox of the CH_4 research community lie within the nonlinear trend of CH_4 mixing ratios in the global atmosphere (Schwietzke et al., 2016; Montzka et al., 2011; National Oceanic & Atmospheric Administration, 2024a). Debates have been raised regarding the contribution sources of CH_4 (the drivers of the atmospheric CH_4 growth) and the high uncertainty of sector-wise CH_4 emission inventories (Rice et al., 2016; Tibrewal et al., 2024; Saunois et al., 2024; Nisbet et al., 2025; Michel et al., 2024; Zhao et al., 2025). Therefore, the identification of CH_4 sources and the quantification of their contributions are essential for solving such puzzle.

The oil and natural gas (ONG) industry is one of the major contributors to anthropogenic CH_4 emissions accounting for approximately 15% of global emissions (Lauvaux et al., 2022). China's ONG industry emerges as potent CH_4 emission sources, which are estimated to contribute 3216.61 Gg in 2024 (International Energy Agency, 2025). However, national-scale estimates remain highly variable and uncertain (Zhang et al., 2014; Sun et al., 2022), largely due to limited observation and poor estimation based on generalized emission factors. Further, the evaluation of CH_4 emission from ONG activities in China is complexed by other strong anthropogenic sources such as agricultural production (e.g., ruminants, rice paddies), wetlands, landfills, and wastewater (Skeie et al., 2023).

Since conventional measurements of CH_4 mixing ratios cannot differentiate among various emission sources, recent studies have applied stable isotope tools for source attribution, based on the distinct isotopic signatures (e.g., $\delta^{13}C\text{-}CH_4$) of microbial and

thermogenic CH_4 (Suzuki, 2021; Peng et al., 2024; Leitner et al., 2020; Dlugokencky et al., 2011). For example, by analyzing the atmospheric $\delta^{13}C$-CH_4 data, Basu et al. (2022) found that microbial sources accounted for 85% of the growth in methane emissions between 2007 and 2016. Another isotope work indicates that CH_4 emissions from the fossil fuel sector remained largely unchanged at the 1980s and 1990s levels, but increased significantly between 2000 and 2009 (Rice et al., 2016). Therefore, isotopic measurements from the atmosphere provides important benchmarks for validating CH_4 contribution from particular sources, and could assist in evaluate CH_4 emission budgets (Michel et al., 2024; Kuhlmann et al., 2025).

For ONG sources, global observations of CH_4 isotopic signatures have yet reached agreement, resulting in large deviations in estimating the source contributions and emission trends (Schwietzke et al., 2016). While the isotope measurement of the background atmosphere sheds light to the global mean source signatures, local measurements of the ground or the lower atmosphere could be more direct in reflecting specific sources such as ONG production or processing. One study has estimated CH_4 emissions from the abandoned ONG wells in the United States, indicating a major contribution from the coalbed and nature gas sources (Townsend-Small et al., 2016). Another research conducted the CH_4 isotopic measurements in the atmosphere over the ONG fields in Romania, confirming the signature from the ONG sources despite a large variation range for $\delta^{13}C$ (Menoud et al., 2022). A recent study revealed that the isotopic characteristics of CH_4 enable differentiation of ONG sources by region and depth, reflecting both the spatial and vertical variability of fossil fuel extraction (Ars et al., 2024). Several researchers used mobile monitoring in Kuwait and identified distinct isotopic signatures from microbial, ONG, and vehicular sources, finding that microbial emissions were the predominant contributor while ONG sources played a relatively minor role (Al-Shalan et al., 2022).

Recent advancements in UAV technology have facilitated novel approaches to monitor and quantify CH_4 emissions, particularly in industrial sites with limited access (Shaw et al., 2021). UAV-based active AirCore systems enable high-resolution sampling and quantification of CH_4 emissions from point sources such as mine

ventilation shafts (Andersen et al., 2023). Combined with inverse Gaussian and mass balance approaches, this method allows effective upscaling to regional emission estimates and has shown high accuracy in the Upper Silesian Coal Basin ($R^2 = 0.7–0.9$). So far, few studies have deployed the UAV method for isotopic determination of methane from ONG site-level (Leitner et al., 2023), and there is a knowledge gap of CH_4 isotopic measurement at the site level considering various factors such as source types (Zhang and Zhu, 2008; Schoell, 1980), processing (e.g., purification or production of light hydrocarbon), meteorological condition, sampling method, size of the site and so on (Liu et al., 2019).

Therefore, to address the CH_4 isotope signatures from Chinese ONG plants and to examine the potential of UAV-based sampling methods, we conducted a field sampling campaign in Sichuan Province, SW China, covering 11 production/processing sites. Vertical profiles (50-300 m) of the air above ONG plants as well as the ground air had been sampled for CH_4 isotopic analyses, in order to provide semi-quantitative understanding of the emission source distributions and to reveal the isotope signatures from local Chinese ONG production and processing activities.

2 Method

2.1 Study sites

The study area is located in Sichuan Basin, Southwest China, where about 19 % of the country's total natural gas reserves have been discovered (The People's Government of Sichuan Province, 2024). Until 2022, the region has about 77,000 km gas pipelines (National Bureau of Statistics, 2024). Between 2013 and 2023, natural gas production in this region increased from 21.31×10^9 to 59.48×10^9 m^3 (Sichuan Provincial Bureau of Statistics, 2024), with an average annual growth rate of about 11%. In 2020, ONG production in Sichuan accounted for 24% of China's total ONG production (National Bureau of Statistics, 2024).

We monitored CH_4 mixing ratios and sampled air for isotope measurements across 11 ONG processing or transportation stations in the central Sichuan Basin. The study region is characterized by a humid subtropical climate, with consistently warm and humid conditions throughout the year. The areas of these stations vary from 2,000 to 300,000 m^2, while the production activities also vary, including natural gas purification plants, gas gathering stations, light hydrocarbon plants, pigging stations, pressurization stations, etc. (Table 1). Most ONG sites are located in remote areas, where the surrounding environment is farmland (paddy fields), bodies of water, forests, and scattered residences, with no large-scale cattle farms, pig manure sites, or landfill sites nearby. In addition, during our observational campaign, no biomass and coal burning has been spotted in the surroundings. For the reasons of privacy and confidentiality, the accurate locations and contours of the ONG stations cannot be disclosed in this paper.

Table 1 Background information of the studied production/processing sites for oil and natural gas

Site	Type	Area (m²)	Processing capacity (10⁴ m³/d)	Surrounding environment	Activity
(S1)	Purification plant	25000	445	Forests, farmland	Natural gas processing, including membrane separation, adsorption, desulfurization, dehydration and other processes
(S2)		113000	3000	Forests, farmland, ponds	
(S3)	Gas gathering stations	9420	278	Forests, farmland	Gas Collection and transportation
(S4)		4220	1000	Farmland, ponds	
(S5)		5096	115	Forests, reservoirs	
(S7)	Light hydrocarbon plant	6650	10	Forests, farmland	C^{3+} component of natural gas was recovered by low temperature separation process
(S8)		25257	30	Forests	
(S9)	Union Station	7958	2700	River	ONG centralized treatment, sewage treatment, product output
(S11)	Supercharging station	7740	24	Farmland, ponds	Pressure and transmission
(S10)	Central well station	8679	90.3	Forests, farmland, ponds	Gas Collection and transportation
(S6)	Pigging station	5167	630	River	

2.2 Sampling methods

From 13 April to 19 April 2023, we monitored and collected samples at 11 ONG production stations in the central Sichuan Basin, obtaining a total of 74 air samples, including 28 from ground and 46 from air overhead. Ground air samples were collected at heights ranging from 0.5 to 2 m above the group. Sampling locations were chosen in

open areas of each station, including areas near pipelines and production equipment. The criteria for selecting the open-ground area includes: no significant elevation in CH_4 concentration compared to the ambient background (Chen et al., 2024), as measured by a portable TDLAS methane analyzer; a minimum distance of 20 meters from any facility; and the absence of visible pipelines or valves. Sampling in the area of pipelines and production equipment was performed at locations that show abnormal mixing ratios after ground monitoring; sampling was performed in the central area if no apparent CH_4 emission was detected. For large sites ($> 10,000 \text{ m}^2$), multiple sampling points were established, while for small sites ($< 10,000 \text{ m}^2$), 1-2 sampling points were established in facility areas, and the sampling time for each sample was about 45-50 seconds.

Air sampling was performed by an Unmanned Aerial Vehicle (UAV) equipped with an automatic sampling pump (Fig. 1). The UAV model was a DJI-T10 upgraded version, and the sampling pump model was KVP04-1.1-12V (1.25 L/min). Taking into account the altitude ranges in previous studies (Kim et al., 2025; Han et al., 2024; Chen et al., 2024; Liu et al., 2021; Liu, 2018; Ali et al., 2017) and the drone's battery life, the monitoring altitudes were defined at 50, 100, 200 and 300 m, respectively. Initially, a ground sampling spot was identified, typically within the pipeline vicinity of the plant. Subsequently, a UAV equipped with an automatic sampling pump and air collection bags were lifted to 300 m above the ground sampling site. The UAV then sequentially descended to altitudes of 200, 100, and 50 m, respectively, dedicating 45 to 60 seconds at each elevation for collecting air samples. This systematic approach ensures a comprehensive and stratified sampling strategy, facilitating the assessment of atmospheric constituents at varying heights.

The volume of each air sample was approximately 1 L, stored in HOONPO Teflon gas bags (1 or 2 L). Air was sampled at varying altitudes from all sites except for S1, which was sampled specifically at 50 m and 100 m. Our sampling was conducted in the daytime between 11:00 am and 2:00 pm. Air sampling and UAV cruising were synchronized. For comparison, we had sampled a production well with significant emissions (built in the 1980s), which was short of maintenance for long. This is meant for directly exploring source signals (2 samples from the leakage point of the well, and

8

180 one sample the open area of the site). In addition, we sampled (2 from the riverbank, 2

181 from the park) ambient air near an urban park and an urban river to analyze the ambient

182 CH_4 mixing ratios and isotope values. The sample list and results are provided in Table
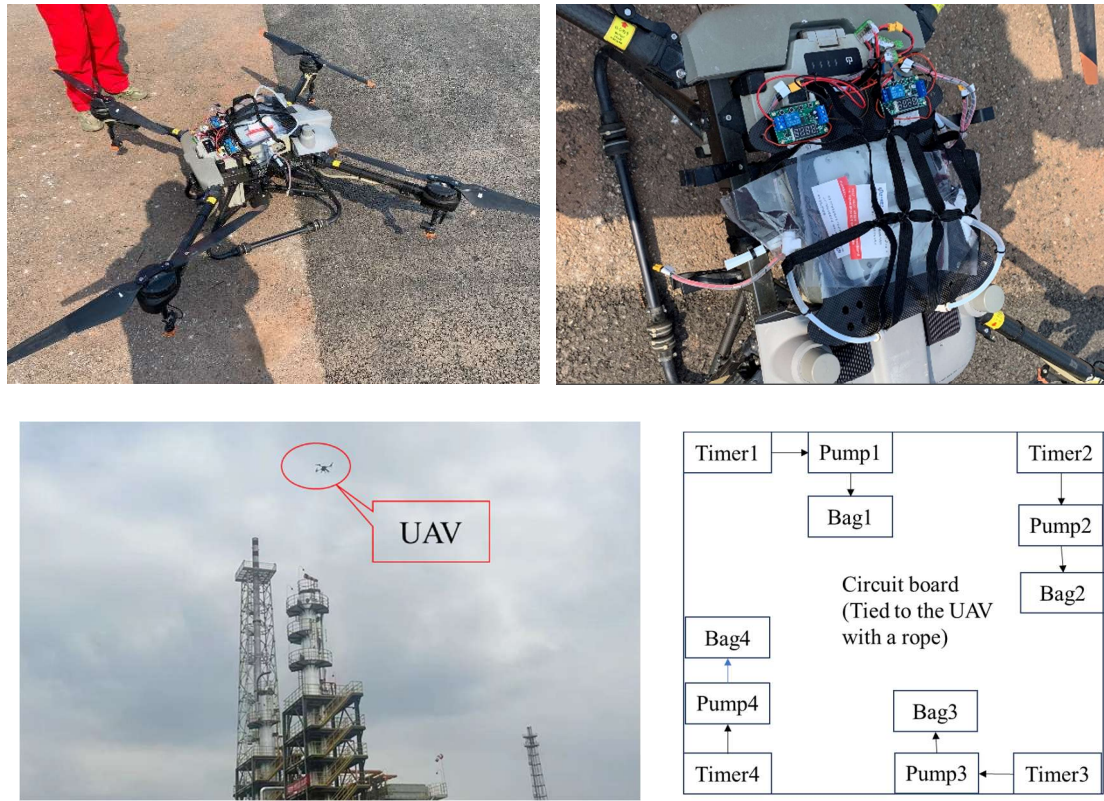
183 S1 (SI).

184

185

186 **Fig. 1** Site demonstration of the UAV automatic sampling system and the schematic

187 diagram of the sampling device.

188 The influence of meteorological conditions on the CH_4 mixing ratios and isotopes at

189 the ONG plants was also considered. Therefore, a portable meteorological station was

190 deployed at each station during the sampling periods. It was equipped with a three-

191 dimensional ultrasonic wind speed and direction sensor (model: M307200), which

192 recorded the wind speed (horizontal and vertical) and direction (horizontal and vertical)

193 near the ground (3 to 10 m according to field conditions). The sampling frequency is

194 32 Hz with a resolution of 0.1 m/s for wind speed and 0.1° for wind direction, and the

195 precision of wind direction and speed is 2° and 0.2 m/s, respectively. We also obtained

196 air pressure, solar radiation, temperature, and relative humidity from weather station.

197 **2.3 Measurement methods**

Gas samples were analyzed within one month after on-site sampling. Picarro G2132-i was used to detect the isotope and mixing ratio of CH_4, which is based on Cavity Ring-Down Spectroscopy (CRDS). This system (in similar models) has been previously used by other studies of in situ CH_4 source characterization (Rella et al., 2015; Lu et al., 2022; Geum et al., 2024). For each sample measurement, the total analysis time is over 180 seconds through the Picarro G2132-i instrument, and the average of the last 120 seconds of CH_4 isotope and mixing ratio data was integrated and exported for raw sample data. We used two international primary standards (VPDB-referenced; Std1 and Std2, -68.6 ‰ and -40.0 ‰, respectively) and one secondary standard (Hstd, -46.89 ‰), all of which had been cross-calibrated (SI, Part 3 for details). During each measurement sequence (SI, Fig. S1), all three standards were measured together with the samples (five samples per sequence). Std1 was used for calibration and for correcting sequence-related drift, Std2 served as a quality control check, and Hstd was used to constrain long-term drift. All measurements were completed within one week after sampling. In addition, repeated measurements of the same isotope standard (Std1) over a year have demonstrated the excellent stability of the instrument (SI, Fig. S2). The $\delta^{13}C$ detection precision (1-σ, 1-hour window) of the instrument is as follows: when the mixing ratio of CH_4 is greater than 1.8 ppm, the precision of 5-minute mean value is better than 0.8 ‰, when the mixing ratio of CH_4 exceeds 10 ppm, the precision is better than 0.4 ‰ (Picarro, 2019).

2.4 Calculation of source isotopic signatures

Based on the sample detection data, the Keeling plot method was used to determine the CH_4 source (Keeling, 1958; Pataki et al., 2003) for each field station, the source isotopic signatures were obtained using a linear regression method based on the least squares approach (France et al., 2016; Akritas and Bershady, 1996). As shown in formula (1):

$$\delta_{(a)} = [CH_{4(b)}] \cdot (\delta_{(b)} - \delta_{(s)}) \cdot 1/[CH_{4(a)}] + \delta_{(s)} \qquad (1)$$

Where $\delta_{(a)}$, $\delta_{(b)}$, and $\delta_{(s)}$ represent the $\delta^{13}C$ values of the sample, the background air and the average source, respectively. $[CH_{4(a)}]$ and $[CH_{4(b)}]$ represent the CH_4 mole

fractions of the sample and the background air, respectively. The intercept ($\delta_{(s)}$) of the fit line is the isotope value of the CH_4 source present in the mixed sample. In linear regression, $1/[CH_{4(a)}]$ and $\delta_{(a)}$ represent independent (X-axis) and dependent (Y-axis) variables, respectively. This method is suitable for carbon dioxide, methane (Thom et al., 1993), water vapor (Moreira et al., 1997), and other gases, but each gas has its specific considerations (Pataki et al., 2003). The gas samples from each station were collected within 30 minutes, during which the atmospheric background values (isotope and mole fraction of CH_4) did not change, fulfilling the application conditions of this method (Lu et al., 2021).

2.5 HYSPLIT model

The Hybrid Single-Particle Lagrange Integrated Trajectory (HYSPLIT) model developed by the National Oceanic and Atmospheric Administration (NOAA) Air Resources Laboratory, is a widely used public platform for different atmospheric scales and supports online modules (Pereira et al., 2019; National Oceanic & Atmospheric Administration, 2024b). The model has been used to calculate the air mass transfer trajectories at different altitudes (Shan et al., 2009; Mcgowan and Clark, 2008; Stein et al., 2015). In the air above ONG plants, ground-based metrological station cannot capture the dynamics of wind directions and speeds. Thus, we deployed the HYSPLIT model to analyze the influence of meteorological conditions on CH_4 mixing ratios and isotopes particularly for the UAV-based sampling and measurements. The time resolution of the model could reach 1 hour and the height resolution was 1 meter. In this study, 24-hour backward trajectories were calculated at each site for five altitudes: ground level, 50 m, 100 m, 200 m, and 300 m. The input data included the longitude and latitude of the site from field measurements and sampling time, while the output information were wind direction and speed at different heights. Additionally, we evaluated the stability indexes based on the HYSPLIT model outputs. It shows that the Pasquill stability classes during UAV sampling was mostly C in our sampling campaigns (Slightly unstable conditions).

2.6 Source partitioning with end-member mixing method

End-member mixing method is a common method for identifying major sources and quantifying contributions of multiple sources (Bugaets et al., 2023; Barthold et al., 2011). The end-member mixing model is conducted with the mass balance of air mixing as well as composition of the tracers, based the following assumptions: (1) the ambient atmospheric constituents are constant, (2) the tracer is conservative, (3) and the source mixing ratios differentiate from the background. Here, we used CH_4 mixing ratios and isotopes as tracers to investigate the contribution of atmospheric background, open surface area, and facility area to the sampled air above various ONG plants.

2.7 Statistics

Data analysis and graphing were performed using Origin 2024 software for Windows. Linear fitting was based on the principle of the least square method, indicating the 0.95 confidence intervals. A value of $P < 0.05$ was considered significant for statistical analysis, and the fitting results are expressed as fitting mean and standard deviation. Maximum, minimum, mean, median, outliers, and 25%-75% range values were also analyzed and reported in the figures or tables.

3 Results

3.1 Variations of CH4 mixing ratios and isotopes across ONG plants

The CH4 mixing ratios and $\delta^{13}C$-CH4 values from the studied 11 ONG sites ranged from 1.88 to 3.66 ppm and from -48.14 to -30.41‰, respectively (SI, Table S1). The maximum and minimum values of CH4 isotopes were observed at sites S2 and S6 (100 m), respectively. The variation of the CH4 mixing ratios and isotopic values at stations S2, S4, and S7 is significantly greater than that observed at other stations (Fig. 2). The results of direct emissions from the production well were -16.19 ± 5.53 ‰ and 118.98 ± 0.52 ppm, respectively. By comparison, the CH4 isotope and mixing ratio of the urban samples were -46.20 ± 0.47 ‰ and 2.04 ± 0.07 ppm, respectively.

More specifically, in the near-ground air, we found higher CH4 mixing ratios and isotopic values in areas close to production equipment than those in the open areas (Fig. 2), although the mixing ratios and isotopic values at S6 and S9 were very similar with the atmospheric background. Overall, the CH4 isotopic values observed from the ground air at the field stations ranged from -47.68 to -16.19 ‰ (-41.99 ± 7.10 ‰ on average), while the isotopic values from the air over plants were more constrained in a small range of -48.14 to -44.11‰.
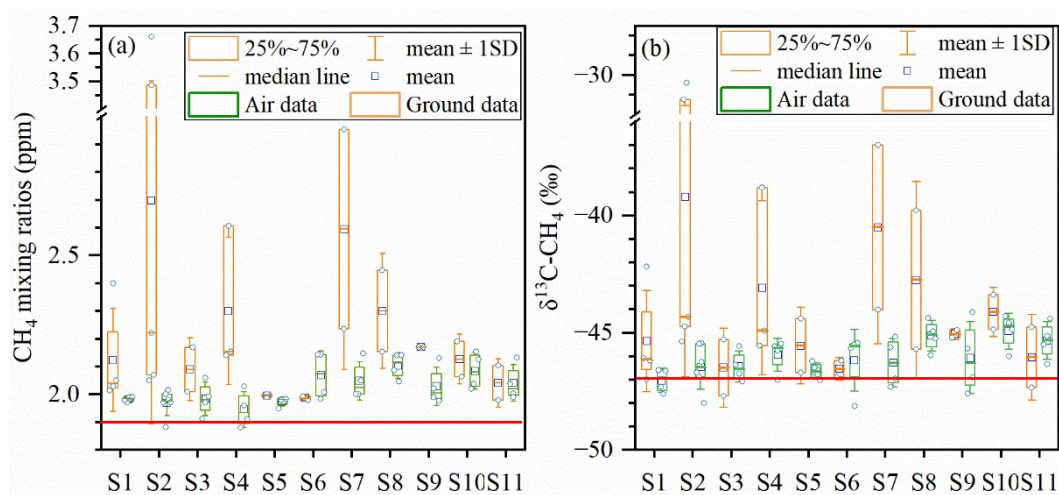

Fig. 2 Box whisker plots of CH4 mixing ratios (a) and isotopic values (b) for air sampled near the plant ground (Ground data) and air sampled above the plants (mean, median, 25% -75% range, and 1 SD are indicated in the figures; the red lines refer to CH4 mixing ratios (a, 1.9 ppm) and isotopic values (b, -47 ‰) from the atmospheric background.

3.2 Vertical profiles of CH₄ mixing ratios and isotopes and source partitioning

The vertical distribution of the CH_4 mixing ratios and isotopes differed from site to site. For instance, the mean CH_4 mixing ratios were higher at 100 m or above than at 50 m, yet the isotopic values ($\delta^{13}C$) were somewhat lower (Fig. 3). From the perspective of each ONG site, the patterns were similar yet more complex (SI, Fig. S3). Some stations exhibited consistent trends (S1, S3, S6, S7, S9, S11), while others displayed different trends (S2, S4, S5, S8, S10). For instance, the CH_4 mixing ratio and isotopic values at 100 m and 200 m altitude of station S8 were inversely proportional. As the altitude increased from the ground to 300 m, the CH_4 isotopic values of stations S4 and S1 exhibited a decline, ranging from -45.47 to -47.00 ‰ (ground to 300 m) and from -42.17 to -47.12 ‰ (ground to 100 m), respectively (SI, Fig. S3). The CH_4 isotopic values of stations S6 initially decreased with increasing altitude and subsequently increased, reaching a minimum at 100 m altitude (-48.14 ‰). The variation of the CH_4 isotope vertical profile at station S8 was analogous to that observed at sites S6, with the exception that the CH_4 isotopic minimum value reached -45.95 ‰ at 200 m altitude. The variation of CH_4 isotopic values with altitude at station S9 was complex, exhibiting a decrease followed by an increase, which then decreased again, reaching minimum and maximum values at 50 m (-47.60 ‰) and 200 m (-44.11‰), respectively.
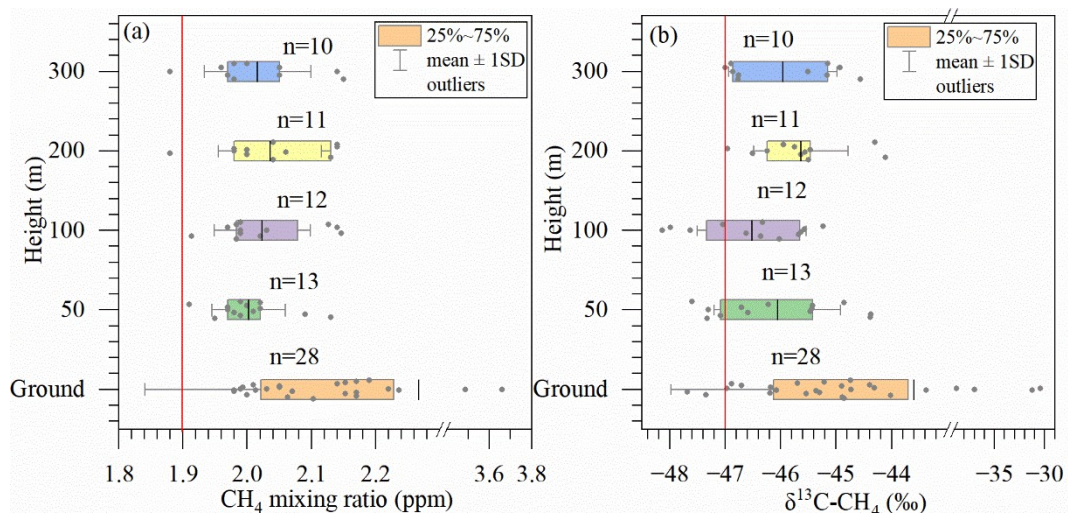

Fig. 3 Box whisker plots showing the variations of CH_4 mixing ratios (a) and isotopic values (b) at different heights (from ground to 300 m at all sites); include mean, 25% - 75% range, and 1 SD; "n" represents the number of samples. The red lines refer to CH_4 mixing ratios (a, 1.9 ppm) and isotopic values (b, -47 ‰) from the atmospheric

322 background.

323

3.3 Source partitioning for CH₄ emission from the ONG plants

The end-member mixing method is a commonly employed technique for calculating isotope mixing by various sources of GHGs (Bugaets et al., 2023). In this study, we determined the contribution fractions of CH_4 from the atmospheric background, surface, and facility areas to the air over the sites (the details and results are presented in SI-part 1, Table S4). The results indicate that atmospheric background is the predominant source of methane, with larger contribution compared with those determined for ground and facility area (Fig. 4). Nevertheless, at altitudes of 100 m, the ground and facility-derived contributions became slightly more important, indicating that these two altitudes may be more representative of the whole-plant emission signals. In particular, at higher altitudes, the signal of CH_4 emissions from ONG plants below may be dampened by mixing of background air or even biological sources in the vicinity of the sites. Despite so, we didn't find any strong emission signals from surrounding environment outside the regions of the ONG plants (no apparent elevation of CH_4 mixing ratios along the vertical profile in the atmosphere).
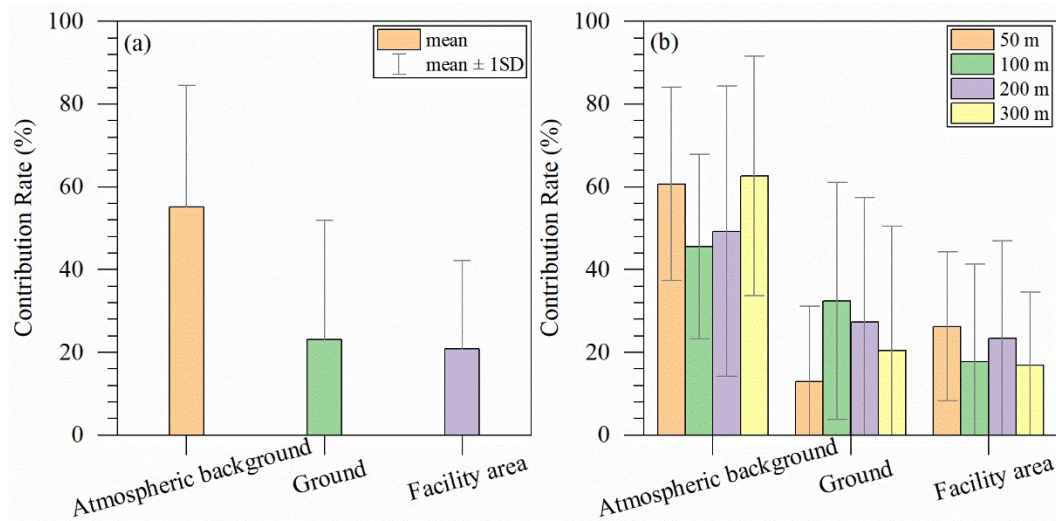

Fig. 4 The fractional contributions from ambient background, surface, and facility areas contribute to the air sampling above ONG plants. (a) the proportion of contributions to all heights of all stations with 1SD; (b) the proportion of contributions to different heights with standard error.

3.4 Characteristics of source isotopes

The Keeling plot method was employed to determine the isotopic signatures (δ^{13}C) of CH$_4$ sources at each station, as presented in Fig. 5. The range of the CH$_4$ source isotopic signatures varied from -52.71 ± 6.06 ‰ to -11.88 ± 2.32 ‰ (mean value of -25.66 ‰), indicating that they were mainly thermogenic sources (associated with oil production) (Menoud et al., 2022; Sherwood Lollar et al., 2002). Globally, the range of CH$_4$ isotopic values from fossil fuels is -75 to -25 ‰ (Defratyka et al., 2021). Our results mostly align with this large range, but were at the higher end.

The source isotopic signature for station S5 was -52.71 ± 6.06 ‰, which was lower than the atmospheric background value. However, the data fitting for this station was poor, indicating large uncertainty (R^2 = 0.08). On the other hand, the direct measurements of emission from wells indicated that source ^{13}C signature was -19.42 ± 2.19 ‰, which is close to the result of the ground-air sample collected in the site (-16.19 ± 5.53 ‰) (SI, Table S1). We conducted continuous monitoring of the natural gas production wells where elevated methane mixing ratios were consistently observed. Given that the sampling was carried out in close proximity to the leakage sources (wells) surrounded by high safety walls, we believe that the derived isotopic signatures could represent the emission source from ONG plants rather than being affected by the surrounding environment.
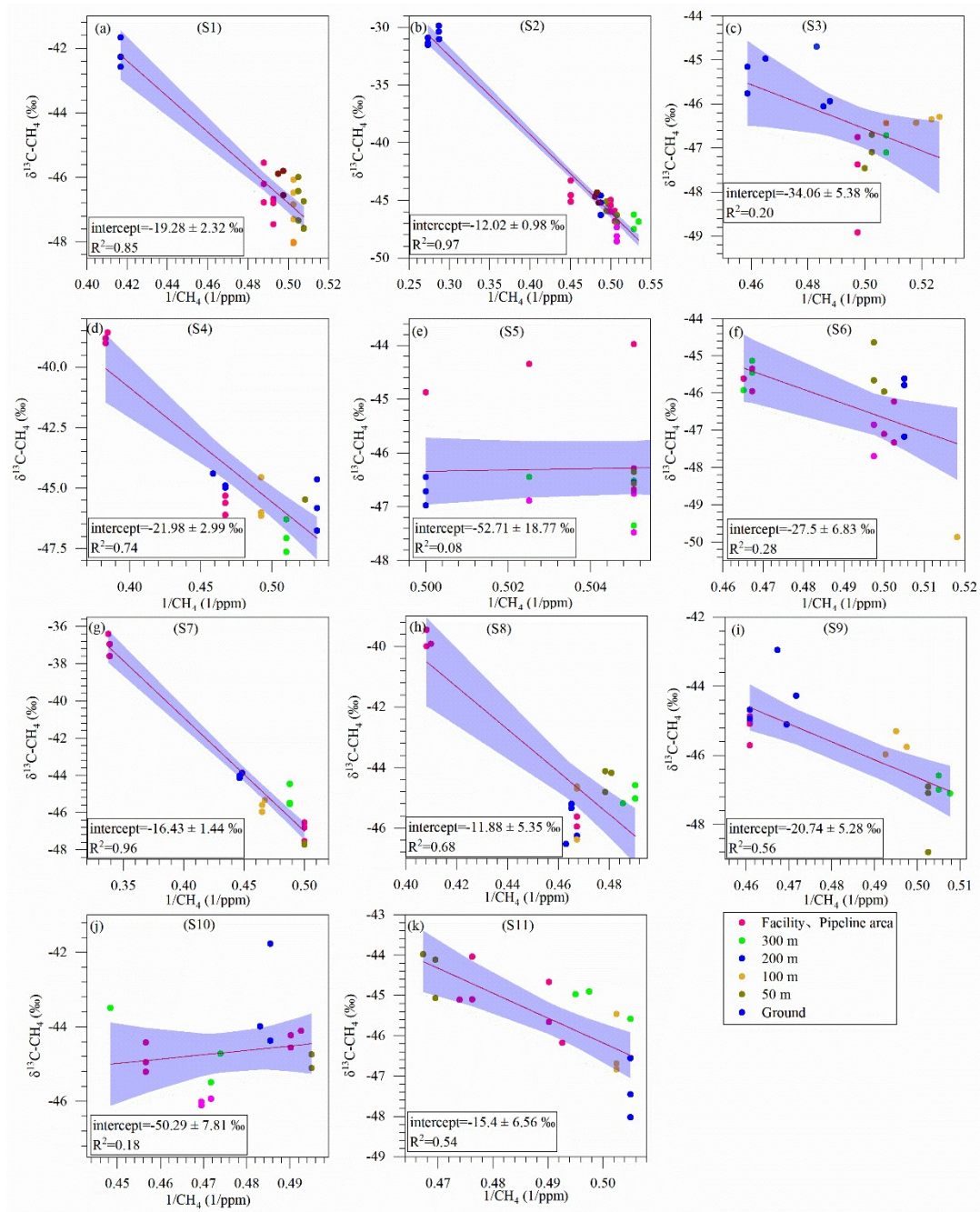
Fig. 5 The CH4 source isotopic signatures of 11 field stations determined based on the Keeling plot method. The blue area represents the 95% confidence interval, and the red line is the result of linear regression posterior mean fit; The samples in different positions are distinguished by different colors. The intercept and R^2 are given, which means the source isotope signal value and the fitting degree, respectively. Linear regression was performed using the least squares method.

4 Discussion

4.1 CH₄ emission signals as revealed by the isotopic measurements from both ground and atmosphere

During our sampling campaign, the mean δ^{13}C-CH$_4$ at most ONG plants was higher than the atmospheric background (-47.0 ± 0.3 ‰) (Tyler, 1986), although several sites (S1, S3, and S5) had values close to the atmospheric background. In the meanwhile, the average values of CH$_4$ mixing ratios were significantly higher than the atmospheric background (1.9 ppm) at all sites (Skeie et al., 2023). This support apparent CH$_4$ leakage from most sites during our study. Further, as refered to the Keeling plot appraoch, the correlation between CH$_4$ mixing ratios and isotopes at the ONG sites was significant ($R^2 = 0.91$) (Fig. 5). Besides, the ground exhibited an even stronger correlation ($R^2 = 0.95$) than the air ($R^2 = 0.31$) (SI, Fig. S4). These findings indicated that the CH$_4$ sources at these ONG plants were generally consistent and reflecting single-source contribution. The δ^{13}C source isotopic signatures from each site may vary, but the major range was consistent with the fossil-fuel sources (Defratyka et al., 2021). In addition, an investigation of the potential sources of CH$_4$ in the vicinity of the ONG sites revealed that the primary source of CH$_4$ at the station was from ONG, with other sources exerting less impact (Table 1).

Further, the variations of δ^{13}C-CH$_4$ across sites may reflect the influence from sources and local facilities. As shown in Fig. 5, the source isotopic signatures determined with the Keeling plot method were distinctively higher in the purification and production sites (S1-S2 and S7-S8) than in the gas gathering and transport lines (S3-S6) (Fig. 5). Studies have indicated that infrastructure, including components such as dehydrators, valves, compressors, and pipelines, represents a significant source of CH$_4$ emissions from the ONG system. Infrastructure is particularly vulnerable to CH$_4$ leakage due to corrosion and wear (Anifowose et al., 2014; Fernandez et al., 2005; Burnham et al., 2012; Anifowose and Odubela, 2015).

On the other hand, sampling locations appears to influence the observational results, particularly when comparing measurements near ground with those made in the air

above (Figs. 2 & 3). We discovered that a majority of the ONG production stations exhibited both higher $\delta^{13}C$ and CH_4 mixing ratios in the ground measurement than in the air at 50-200 m aboveground (Fig. 3). This suggests that ground-based measurements are likely to exert more significant source signals when CH_4 leakage occurs nearby. However, this may only apply to small ONG sites. Alternatively, measurements of air above the plants could provide information on the site-level emission, of which 100 m (on average) seems to perform best in representing emission signals as confirmed by the end-member analyses (Fig. 4) according to the local settings. By contrast, the mixing ratios and $\delta^{13}C$ of CH_4 at S6 were lower in the near-ground air than in the air overhead. This discrepancy may be attributed to the uncertainty associated with the small plant size (5167 m^2 with a processing capacity of 630×10^4 m^3/d) and thus large impact from surrounding environment sources of CH_4 in the air. Therefore, the surrounding emission sources, together with the metrological conditions, are likely to exert an impact on the UAV-based measurements considering local conditions of the ONG plants.

4.2 Factors of drone-based isotope measurements in the atmosphere

As shown in Figs. 2, 3 and 4, a wide range was found for the CH_4 mixing ratios and isotopic values determined at the studied ONG plants, with particular variabilities observed at varying altitudes above ground. This could be attributed to a number of factors, including the presence of other CH_4 sources in the vicinity and the influence of meteorological conditions (Kavitha and Nair, 2016). Around all ONG sites, the dominant land-use types are rural roads and scattered paddy fields, through which small ditches or streams flow. No livestock farm or landfill was observed in these areas, and no biomass burning was observed during our sampling period (April), which aligns with the legal prohibition of such activities in China. Taking this evidence into consideration, we can rule out the possibility of significant contributions from biological sources from the surrounding environment. The dampened signals of both CH_4 mixing ratios and isotopes in the air-borne measurements may be partly due to convection with air carrying biological sources outside the range of the ONG plants,

but the overall strength is small as confirmed with the Keeling plots (Fig. 5). Further, at station S6 where the 200-300 m-measurement exhibited high CH_4 levels, we also found higher $\delta^{13}C$, which does not support the importance of biological sources which is usually characterized with lower $\delta^{13}C$ (Fisher et al., 2011 & 2017).

Importantly, our UAV sampling points were mostly located near the center or at least away from the edges of the ONG sites, which are significantly larger in area compared to the scattered paddy fields nearby. The Pasquill stability class during the sampling indicated slightly unstable atmospheric conditions, suggesting predominant vertical mixing over horizontal transport. This enhances the reliability of isotopic measurements in reflecting methane emissions from the station itself, with the ONG site being the primary source influencing the isotopic signatures. Furthermore, in a parallel study conducted by our team in the same region (Chen et al., 2024), several ambient air samples were collected for $\delta^{13}C$-CH_4 analysis near paddy fields (1.5 meters above the surface, 10–20 meters from field boundaries). The isotopic values ($\delta^{13}C$-CH_4 = -47.2 ± 0.2 ‰; unpublished data) were quite close to the global background, indicating minimal influence from the paddy fields. This could be attributed to the relatively low methane emissions during the sampling period, as April is typically dry in the Sichuan region.

The influence of meteorological conditions is significant and complex, and challenging to analyze. Wind direction and speed in the air above plants were obtained using the HYSPLIT model (SI, Table S3), and the results for near-ground air were cross-validated with that obtained from the meteorological station (SI, Fig. S5). The correlation analysis between wind speed and CH_4 isotope results revealed an exponential relationship with a R-squared value of 0.33 (SI, Fig. S6). This indicates that as wind speed increases, the impact of CH_4 diffusion and dilution becomes more significant. Wind direction plays a role in the uncertainty of CH_4 distribution, as it has a significant influence on CH_4 transport near the surface, resulting in a non-uniform distribution of CH_4 and typically higher mixing ratios downwind from the emission source. Furthermore, upwind CH_4 sources can have a notable impact on CH_4 levels over the station. The utilization of HYSPLIT model serves a crucial function in this regard (SI, Fig. S7 for a detailed example of S7 site).

462 Moreover, the local conditions of the ONG plants are among the primary determining

463 factors of the air-borne measurements, encompassing factors such as the size of the sites,

464 the treatment processes employed, the processing capacity, and the timing and location

465 of sampling. Typically, a larger site size is likely to produce greater signals of CH_4 in

466 the atmosphere above head and to be less affected by other biological sources from

467 surrounding environment (Omara et al., 2016). A clear positive correlation was

468 observed between the site area and the isotope results for site areas below 10,000 m^2

469 (SI, Fig. S8). This is interesting and probably also reasonable, as extra-large industrial

470 sites may encompass more complexed influence from both metrological conditions and

471 ground source distributions. Besides, the intermittent nature of emissions from the site

472 facilities introduces an element of uncertainty with regard to the sampling time and

473 locations (Omara et al., 2016). Overall, by conducting a simple Principal Component

474 Analysis (PCA), we identified a weak relationship among wind direction, wind speed

475 and isotopes, and a strong correlation between the size and capacity of the sites with

476 CH_4 isotopes (SI, Fig. S9). This means that, during our sampling campaign, ONG plant-

477 related factors are the major players in determining the measured CH_4 isotope results.

478

479 **4.3 Global source isotopic signatures of ONG-derived CH_4**

480 While no studies have specifically focused on the isotopic characteristics of CH_4

481 leakage from ONG plants in Sichuan region of China, several studies have investigated

482 the characteristics of CH_4 isotopes in Chinese ONG production regions, across the

483 Sichuan Basin, Xinjiang, Northeastern China, and the Ordos Basin (Cai et al., 2013;

484 Huang et al., 2017; Wang et al., 2018; Zhang et al., 2018; Zou et al., 2007; Zhu et al.,

485 2014; Liu et al., 2019; Dai et al., 1985; Dai et al., 1992; Xu, 1994). The reported values

486 of CH_4 isotopes cover a wide range from -54.9 to -17.4 ‰ (SI, Table S2). The difference

487 in ^{13}C-CH_4 reflects the origin of natural gas such as biogenic and abiogenic gases

488 (Sherwood Lollar et al., 2002; Dai et al., 2005), of which biogenic gases include coal-

489 and oil-type gases, respectively. The Sichuan Basin in our study has a complex

490 geological environment and many gas-production layers, such as Cambrian, Ordovician,

491 Carboniferous, Jurassic and so on (Zhang et al., 2018; Cai et al., 2013); also, CH_4 from

different geological layers can have variable isotopic characteristics. In comparison with the findings of other researchers on CH_4 isotopes in the Sichuan Basin (SI, Table S2), our results of ^{13}C-CH_4 isotope signatures spanned more widely and appeared to be generally heavier (Fig. 5).

Among the global observations, Menoud et al. examined isotopic signatures of CH_4 from an ONG extraction plant in Romania. Their methodology aligns closely with ours, and their findings indicate a range of $\delta^{13}C$ values from -67.8 ± 1.2 ‰ to -22.4 ± 0.04 ‰ (Menoud et al., 2022). In Kuwait, methane from the southern Burgan field had a $\delta^{13}C$-CH_4 of -48.9 ± 0.2 ‰, and the signals were slighter lower by measuring downwind of coastal refineries (-51.6 ± 0.5 ‰) (Al-Shalan et al., 2022). A study on CH_4 isotopes in the Western Canadian Sedimentary Basin showed that the $\delta^{13}C$ signatures of CH_4 from ONG sources ranged between -71 ‰ and -29.3 ‰, and the isotopic composition was primarily controlled by geological structure rather than the type of hydrocarbon (e.g., ONG sources) (Ars et al., 2024). In an Arctic study, Fisher et al. (Fisher et al., 2011) found that CH_4 in the Arctic atmosphere during summer is mainly of microbial origin, whereas in spring and winter, the dominant source is likely CH_4 emissions from natural gas fields, with a source $\delta^{13}C$-CH_4 signature of -52.6 ± 6.4 ‰. In the UK, $\delta^{13}C$–CH_4 signatures from ONG sources were well constrained, showing consistent values of approximately -36 ± 2 ‰, reflecting homogenized North Sea gas (Zazzeri et al., 2015). Compared with those previous work on ONG-related CH_4 sources, our results are overlapping with the wide ranges as reported; the overall mean values are heavier and well above the global mean of fossil fuel CH_4 isotope (-44.0 ± 0.7 ‰) (Michel et al., 2024). This discrepancy can be attributed to a number of factors, including thermogenic origin, geographical differences (Menoud et al., 2022), the treatment processing of natural gas, and likely uncertainty due to limited sample size.

The methane isotopic signatures observed in this study were compared with those reported from major ONG production regions world widely (Fig. 6). The $\delta^{13}C$ of CH_4 was found to be lighter in the United States and Canada, but heavier in China. Regional variations in $\delta^{13}C$ values were observed, even within the same region (e.g. in China). Our results exhibited a significantly heavier $\delta^{13}C$ than those of other studies. This is

522   most likely to be attributed to differences in the origin of CH_4 (Zhang and Zhu, 2008;

523   Wang et al., 2018; Defratyka et al., 2021; Schoell, 1980), as we have excluded the

524   possibility of strong influence from biological sources or biomass burning in the
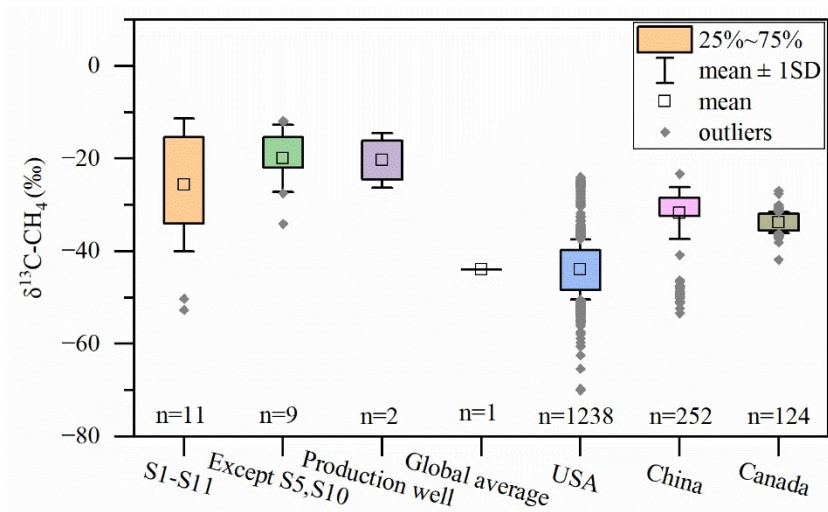
525   surrounding environment as discussed above.

526

Fig. 6 Comparison of CH_4 isotopic signatures in oil and natural gas production regions
across major hydrocarbon-producing countries; data from both literature and this study
are included. The number of data points is shown at the bottom of the box chart, and
carry on the error analysis. "n" represents the number of data points.

531

532   The $\delta^{13}C$ of CH_4 represents a valuable indicator for constraining and estimating CH_4

533   emissions particularly from anthropogenic sources of the globe (Milkov et al., 2020).

534   As a sum-up, the mean $\delta^{13}C$ signatures of CH_4 sources as indicated from measurements

535   of atmospheric background integrated the collective contributions from various sources

536   of CH_4. Hence, with the updated isotopic signatures for specific sources such as ONG

537   industry, the previous conclusions on global contribution/flux of CH_4 from ONG

538   industry may need to be revised (Schwietzke et al., 2016). In comparison with previous

539   studies, the $\delta^{13}C$ values from ONG industry in our work (-25.66 ‰, mean values of the

540   11 stations) are higher, especially different from the global flux-weighted averaged by

541   Schwietzke et al. (Schwietzke et al., 2016). By incorporation of flux contribution from

542   Chinese ONG industry, isotope signatures as well as global datasets utilized in the

543   previous work (Schwietzke et al., 2016), we conducted a sensitivity analysis, examining

544   the effect on diverse source contributions (in flux) when updated the $\delta^{13}C$-CH_4 from

545   Chinese ONG industry (SI, part 2 for details).

546   Our finding suggests that, the updated ^{13}C isotope signature based on field

547 observation from China would elevate global fossil fuel-derived CH_4 isotopes signature

548 by about 0.46 ‰; as a consequence, the new result would lead to a smaller contribution

549 from global ONG industry (corresponds to an overestimation of emissions by 2.86 Tg

550 CH_4 yr^{-1}) but a larger contribution from microbial sources. This finding is consistent

551 with some recent research findings, such as Chandra et al. (Chandra et al., 2024), who

552 reported that CH_4 emissions decreased in fossil fuel sources, while increasing in

553 microbial sources during 1990-2020. In Australia, CH_4 emissions from agricultural

554 ponds, which are microbial in origin, have been underestimated in national greenhouse

555 gas inventories, indicating that actual CH_4 emissions may be higher than officially

556 reported (Malerba et al., 2022).

557

558 **4.4 Feasibility and limitations**

559   Atmosphere CH_4 isotopic research has shown its power in distinguishing between

560 microbial and fossil sources of global atmospheric CH_4 trends (Basu et al., 2022;

561 Bruhwiler et al., 2017). However, due to scarcity of observational evidence of various

562 CH_4 source signatures, large uncertainties still exist for such estimations. The objective

563 of our research was to distinguish sources of CH_4 as well as to indicate CH_4 leakage

564 strength at site-level, providing basic but convincing information for constraining CH_4

565 leakage. With both ground- and air-based approaches, our study has demonstrated the

566 feasibility of our sampling method and research design in studying the characteristics

567 of CH_4 sources and their influencing factors at ONG stations in SW China. Nevertheless,

568 it is necessary to point out, that the impact of meteorological conditions and site

569 conditions on the dampening/masking of CH_4 isotope signatures in the atmosphere

570 cannot be neglected, particularly considering the limited sampling sizes during our

571 campaign. Therefore, the reconciliation between ground-based and atmospheric

572 measurements as well as source partitioning remain to be further validated, given more

573 sampling coverage both spatially and temporally. In addition, more sampling at

574 different locations or different ONG plants will be greatly beneficial to better confirm

575 the CH_4 source isotope signature from fossil fuel industry in China.

576   Recently, the debates on the global atmospheric trends of CH_4 levels and the driving

577   sources are continuing (Saunois et al., 2024; Kirschke et al., 2013; Rice et al., 2016;

578   Tibrewal et al., 2024). Overall, the decline of global mean CH_4 isotopic signals seem to

579   slightly speed up in recent years, likely supporting the importance of microbial

580   emissions (Nisbet et al., 2016). The atmospheric chemists have recently clarified the

581   important link of air pollutants with atmospheric CH_4 sink strengths, further

582   complicating the story. For the ONG industry, previous studies have reported

583   improvements in technology, equipment, and management practices which will assist

584   for reducing CH_4 leakage (US Environmental Protection Agency, 2012; China National

585   Petroleum Corporation, 2023). Therefore, the contribution from ONG sources to the

586   global CH_4 budget is likely to decline. With more field observation and more up-to-date

587   database being established, we would be able to pursue a more realistic evaluation of

588   ONG-contributed CH_4 emission inventory, providing guidance on further mitigation

589   measures.

5 Summary

In this study, we examined the $\delta^{13}C$ isotopic characteristics of air samples collected from ONG stations in the central Sichuan Basin, China. The CH_4 isotopes were measured near the ground and in the air along a vertical profiles of altitudes. By comparing isotopic results across sites and among sampling locations, we found that source distributions by industrial facilities as well as processing capacity/site sizes act as the major driving factors of CH_4 mixing ratios and isotopic signals, while the influence from meteorological conditions and other sources from the surrounding environment may exert less impact. Based on the Keeling plot method, we determined that the source $\delta^{13}C$ signature of CH_4 from the ONG sites ranged was -25.66 ‰, indicating a heavy $\delta^{13}C$ of fossil fuel. In comparison with the CH_4 isotopic values from the global ONG sources, our study reported generally heavier isotopic signatures. By updating the isotope signatures of Chinese ONG with our observation, we conducted a weighted calculation of flux and isotope for the global CH_4 budget, suggesting that the global CH_4 emissions from microbial sources may be underestimated, while those from fossil fuel sources may be overestimated. Overall, our study confirms the effectiveness of isotope method in distinguishing industrial CH_4 sources and sheds light to the global estimation of CH_4 budgets utilizing the isotope geochemistry approach.

Acknowledgements

Author contributions

D. Chen and Y. Liu conceptualized the study, with guidance from L. Yu., D. Chen and Y. Liu conducted the field observation and sample analysis, with the help from Z. Niu, A. Wang and X. Pang. Y. Huang contributed data for the global literature analysis. D. Chen, Y. Liu and L. Yu wrote the manuscript together. All coauthors reviewed and contributed to the revision and finalization of the manuscript.

Competing interests

The authors declare no competing interests.

Data availability

All the data published in this work could be accessed upon request from the corresponding author.

References

Akritas, M. G. and Bershady, M. A.: Linear Regression for Astronomical Data with Measurement Errors and Intrinsic Scatter, The Astrophysical Journal, 470, 177901, 1996.

Al-Shalan, A., Lowry, D., Fisher, R. E., Nisbet, E. G., Zazzeri, G., Al-Sarawi, M., and France, J. L.: Methane emissions in Kuwait: Plume identification, isotopic characterisation and inventory verification, Atmospheric Environment, 268, 118763, 2022.

Ali, H., Odeh, M., Odeh, A., Abou-ElNour, A. A., and Tarique, M.: Unmanned Aerial Vehicular System for Greenhouse Gas Measurement and Automatic Landing, Netw. Protoc. Algorithms, 9, 56-76, 2017.

Andersen, T., Zhao, Z., de Vries, M., Necki, J., Swolkien, J., Menoud, M., Röckmann, T., Roiger, A., Fix, A., Peters, W., and Chen, H.: Local-to-regional methane emissions from the Upper Silesian Coal Basin (USCB) quantified using UAV-based atmospheric measurements, Atmos. Chem. Phys., 23, 5191-5216, 2023.

Anifowose, B. and Odubela, M.: Methane emissions from oil and gas transport facilities – exploring innovative ways to mitigate environmental consequences, Journal of Cleaner Production, 92, 121-133, 2015.

Anifowose, B., Lawler, D., van der Horst, D., and Chapman, L.: Evaluating interdiction of oil pipelines at river crossings using Environmental Impact Assessments, Area, 46, 4-17, 2014.

Ars, S., Arismendi, G. G., Muehlenbachs, K., Worthy, D. E. J., and Vogel, F.: Using in situ measurements of $\delta^{13}C$ in methane to investigate methane emissions from the western Canada sedimentary basin, Atmospheric Environment: X, 23, 100286, 2024.

Barthold, F. K., Tyralla, C., Schneider, K., Vaché, K. B., Frede, H.-G., and Breuer, L.: How many tracers do we need for end member mixing analysis (EMMA)? A sensitivity analysis, Water Resources Research, 47, 2011.

Basu, S., Lan, X., Dlugokencky, E., Michel, S., Schwietzke, S., Miller, J. B., Bruhwiler, L., Oh, Y., Tans, P. P., and Apadula, F.: Estimating emissions of methane consistent with atmospheric measurements of methane and $\delta^{13}C$ of methane, Atmospheric Chemistry and Physics Discussions, 2022, 1-38, 2022.

Bruhwiler, L. M., Basu, S., Bergamaschi, P., Bousquet, P., Dlugokencky, E., Houweling, S., Ishizawa, M., Kim, H.-S., Locatelli, R., Maksyutov, S., Montzka, S., Pandey, S., Patra, P. K., Petron, G., Saunois, M., Sweeney, C., Schwietzke, S., Tans, P., and Weatherhead, E. C.: U.S. CH4 emissions from oil and gas production: Have recent large increases been detected?, Journal of Geophysical Research: Atmospheres, 122, 4070-4083, 2017.

Bugaets, A., Gartsman, B., Gubareva, T., Lupakov, S., Kalugin, A., Shamov, V., and Gonchukov, L.: Comparing the Runoff Decompositions of Small Experimental Catchments: End-Member Mixing Analysis (EMMA) vs. Hydrological Modelling, Water, 15, 752, 2023.

Burnham, A., Han, J., Clark, C. E., Wang, M., Dunn, J. B., and Palou-Rivera, I.: Life-cycle greenhouse gas emissions of shale gas, natural gas, coal, and petroleum, Environmental science & technology, 46, 619-627, 2012.

Cai, C., Zhang, C., He, H., and Tang, Y.: Carbon isotope fractionation during methane-dominated TSR in East Sichuan Basin gasfields, China: A review, Marine and Petroleum Geology, 48, 100-110, 2013.

Chandra, N., Patra, P. K., Fujita, R., Höglund-Isaksson, L., Umezawa, T., Goto, D., Morimoto, S.,

Vaughn, B. H., and Röckmann, T.: Methane emissions decreased in fossil fuel exploitation and sustainably increased in microbial source sectors during 1990–2020, Communications Earth & Environment, 5, 147, 2024.

Chen, L., Pang, X., Wu, Z., Huang, R., Hu, J., Liu, Y., Zhou, L., Zhou, J., and Wang, Z.: Unmanned aerial vehicles equipped with sensor packages to study spatiotemporal variations of air pollutants in industry parks, Philosophical Transactions of the Royal Society A: Mathematical, Physical and Engineering Sciences, 382, 20230314, doi:10.1098/rsta.2023.0314, 2024.

"Intelligent" control of methane emission by digital module in southwest oil and gas field: http://news.cnpc.com.cn/system/2023/12/22/030121011.shtml, last access: 12 June 2025.

Dai, J., Pei, X., and Qi, H.: Natural gas geology in China, Petroleum Publication, 42-46, 1992.

Dai, J., Qi, H., and Song, Y.: Primary discussion of some parameters for identification of coal-and oil-type gases, Acta Petrolei Sinica, 6, 31-38, 1985.

Dai, J., Yang, S., Chen, H., and Shen, X.: Geochemistry and occurrence of inorganic gas accumulations in Chinese sedimentary basins, Organic Geochemistry, 36, 1664-1688, 2005.

Defratyka, S. M., Paris, J.-D., Yver-Kwok, C., Fernandez, J. M., Korben, P., and Bousquet, P.: Mapping Urban Methane Sources in Paris, France, Environmental Science & Technology, 55, 8583-8591, 2021.

Dlugokencky, E. J., Nisbet, E. G., Fisher, R., and Lowry, D.: Global atmospheric methane: budget, changes and dangers, Philosophical Transactions of the Royal Society A: Mathematical, Physical and Engineering Sciences, 369, 2058-2072, 2011.

Energy Resources: https://www.sc.gov.cn/10462/10778/10876/2021/1/4/abbdfe3e4cb943d885236f623361caf7.s html#:~:text=%E6%B2%B9%E6%B0%94%E8%B5%84%E6%BA%90%E4%BB%A5%E5 %A4%A9%E7%84%B6%E6%B0%94,%E5%8C%BA%E3%80%81%E5%B7%9D%E4%B 8%9C%E5%8C%97%E7%89%87%E5%8C%BA%E3%80%82, last access: 12 June 2025.

Fernandez, R., Petrusak, R., Robinson, D., and Zavadil, D.: Cost-Effective Methane Emissions Reductions for Small and Midsize Natural Gas Producers, Journal of Petroleum Technology, 57, 34-42, 2005.

Fisher, R. E., Sriskantharajah, S., Lowry, D., Lanoisellé, M., Fowler, C. M. R., James, R. H., Hermansen, O., Lund Myhre, C., Stohl, A., Greinert, J., Nisbet-Jones, P. B. R., Mienert, J., and Nisbet, E. G.: Arctic methane sources: Isotopic evidence for atmospheric inputs, Geophysical Research Letters, 38, 2011.

Fisher, R. E., France, J. L., Lowry, D., Lanoisellé, M., Brownlow, R., Pyle, J. A., Cain, M., Warwick, N., Skiba, U. M., Drewer, J., Dinsmore, K. J., Leeson, S. R., Bauguitte, S. J.-B., Wellpott, A., O'Shea, S. J., Allen, G., Gallagher, M. W., Pitt, J., Percival, C. J., Bower, K., George, C., Hayman, G. D., Aalto, T., Lohila, A., Aurela, M., Laurila, T., Crill, P. M., McCalley, C. K., and Nisbet, E. G.: Measurement of the ^{13}C isotopic signature of methane emissions from northern European wetlands, Global Biogeochemical Cycles, 31, 605-623, 2017.

France, J. L., Cain, M., Fisher, R. E., Lowry, D., Allen, G., O'Shea, S. J., Illingworth, S., Pyle, J., Warwick, N., Jones, B. T., Gallagher, M. W., Bower, K., Le Breton, M., Percival, C., Muller, J., Welpott, A., Bauguitte, S., George, C., Hayman, G. D., Manning, A. J., Myhre, C. L., Lanoisellé, M., and Nisbet, E. G.: Measurements of δ^{13}C in CH_4 and using particle dispersion

modeling to characterize sources of Arctic methane within an air mass, Journal of Geophysical Research: Atmospheres, 121, 14,257-214,270, 2016.

Han, T., Xie, C., Yang, Y., Zhang, Y., Huang, Y., Liu, Y., Chen, K., Sun, H., Zhou, J., Liu, C., Guo, J., Wu, Z., and Li, S.-M.: Spatial mapping of greenhouse gases using a UAV monitoring platform over a megacity in China, Science of The Total Environment, 951, 175428, 2024.

Hmiel, B., Petrenko, V. V., Dyonisius, M. N., Buizert, C., Smith, A. M., Place, P. F., Harth, C., Beaudette, R., Hua, Q., Yang, B., Vimont, I., Michel, S. E., Severinghaus, J. P., Etheridge, D., Bromley, T., Schmitt, J., Faïn, X., Weiss, R. F., and Dlugokencky, E.: Preindustrial $^{14}CH_4$ indicates greater anthropogenic fossil CH_4 emissions, Nature, 578, 409-412, 2020.

Huang, S., Feng, Z., Gu, T., Gong, D., Peng, W., and Yuan, M.: Multiple origins of the Paleogene natural gases and effects of secondary alteration in Liaohe Basin, northeast China: Insights from the molecular and stable isotopic compositions, International Journal of Coal Geology, 172, 134-148, 2017.

Intergovernmental Panel on Climate Change: Climate Chang 2021 The Physical Science Basis, 1017, 2021.

G2132-i Isotope Analyzer: https://www.picarro.com/sites/default/files/product_documents/Picarro_G2132-i%20Chinese%20Datasheet.pdf, last access: 12 June 2025.

Geum, S., Park, H., Choi, H., Kim, Y., Lee, H., Joo, S., Oh, Y.-S., Michel, S. E., and Park, S.: Identifying emission sources of CH_4 in East Asia based on in-situ observations of atmospheric $\delta^{13}C$-CH_4 and C_2H_6, Science of The Total Environment, 908, 168433, 2024.

Global Methane Tracker 2025: https://www.iea.org/reports/global-methane-tracker-2024, last access: 12 June 2025.

Kavitha, M. and Nair, P. R.: Non-homogeneous vertical distribution of methane over Indian region using surface, aircraft and satellite based data, Atmospheric Environment, 141, 174-185, 2016.

Keeling, C. D.: The concentration and isotopic abundances of atmospheric carbon dioxide in rural areas, Geochimica et Cosmochimica Acta, 13, 322-334, 1958.

Kim, H., Kim, K. T., Jeong, S., Lee, Y. S., Zhao, X., and Kim, J. Y.: Enhancing Uncrewed Aerial Vehicle Techniques for Monitoring Greenhouse Gas Plumes at Point Sources, Atmospheric Environment, 342, 120924, 2025.

Kirschke, S., Bousquet, P., Ciais, P., Saunois, M., Canadell, J. G., Dlugokencky, E. J., Bergamaschi, P., Bergmann, D., Blake, D. R., Bruhwiler, L., Cameron-Smith, P., Castaldi, S., Chevallier, F., Feng, L., Fraser, A., Heimann, M., Hodson, E. L., Houweling, S., Josse, B., Fraser, P. J., Krummel, P. B., Lamarque, J.-F., Langenfelds, R. L., Le Quéré, C., Naik, V., O'Doherty, S., Palmer, P. I., Pison, I., Plummer, D., Poulter, B., Prinn, R. G., Rigby, M., Ringeval, B., Santini, M., Schmidt, M., Shindell, D. T., Simpson, I. J., Spahni, R., Steele, L. P., Strode, S. A., Sudo, K., Szopa, S., van der Werf, G. R., Voulgarakis, A., van Weele, M., Weiss, R. F., Williams, J. E., and Zeng, G.: Three decades of global methane sources and sinks, Nature Geoscience, 6, 813-823, 2013.

Kuhlmann, G., Stavropoulou, F., Schwietzke, S., Zavala-Araiza, D., Thorpe, A., Hueni, A., Emmenegger, L., Calcan, A., Röckmann, T., and Brunner, D.: Evidence of successful methane mitigation in one of Europe's most important oil production region, Atmos. Chem. Phys., 25, 5371-5385, 10.5194/acp-25-5371-2025, 2025.

Lauvaux, T., Giron, C., Mazzolini, M., d'Aspremont, A., Duren, R., Cusworth, D., Shindell, D., and Ciais, P.: Global assessment of oil and gas methane ultra-emitters, Science, 375, 557-561, 2022.

Leitner, S., Hood-Nowotny, R., and Watzinger, A.: Successive and automated stable isotope analysis of CO_2, CH_4 and N_2O paving the way for unmanned aerial vehicle-based sampling, Rapid Communications in Mass Spectrometry, 34, e8929, 2020.

Leitner, S., Feichtinger, W., Mayer, S., Mayer, F., Krompetz, D., Hood-Nowotny, R., and Watzinger, A.: UAV-based sampling systems to analyse greenhouse gases and volatile organic compounds encompassing compound-specific stable isotope analysis, Atmospheric Measurement Techniques, 16, 513-527, 2023.

Liu, Q., Wu, X., Wang, X., Jin, Z., Zhu, D., Meng, Q., Huang, S., Liu, J., and Fu, Q.: Carbon and hydrogen isotopes of methane, ethane, and propane: A review of genetic identification of natural gas, Earth-Science Reviews, 190, 247-272, 2019.

Liu, S.: Development of a UAV-based system to monitor air quality over an oil field, Montana Tech of The University of Montana, 2018.

Liu, S., Yang, X., and Zhou, X.: Development of a low-cost UAV-based system for CH4 monitoring over oil fields, Environmental Technology, 42, 3154-3163, 10.1080/09593330.2020.1724199, 2021.

Lu, X., Harris, S. J., Fisher, R. E., France, J. L., Nisbet, E. G., Lowry, D., Röckmann, T., van der Veen, C., Menoud, M., Schwietzke, S., and Kelly, B. F. J.: Isotopic signatures of major methane sources in the coal seam gas fields and adjacent agricultural districts, Queensland, Australia, Atmos. Chem. Phys., 21, 10527-10555, 2021.

Malerba, M. E., de Kluyver, T., Wright, N., Schuster, L., and Macreadie, P. I.: Methane emissions from agricultural ponds are underestimated in national greenhouse gas inventories, Communications Earth & Environment, 3, 306, 2022.

McGowan, H. and Clark, A.: Identification of dust transport pathways from Lake Eyre, Australia using Hysplit, Atmospheric Environment, 42, 6915-6925, 2008.

Menoud, M., van der Veen, C., Maazallahi, H., Hensen, A., Velzeboer, I., van den Bulk, P., Delre, A., Korben, P., Schwietzke, S., Ardelean, M., Calcan, A., Etiope, G., Baciu, C., Scheutz, C., Schmidt, M., and Röckmann, T.: CH4 isotopic signatures of emissions from oil and gas extraction sites in Romania, Elementa: Science of the Anthropocene, 10, 2022.

Michel, S. E., Lan, X., Miller, J., Tans, P., Clark, J. R., Schaefer, H., Sperlich, P., Brailsford, G., Morimoto, S., Moossen, H., and Li, J.: Rapid shift in methane carbon isotopes suggests microbial emissions drove record high atmospheric methane growth in 2020–2022, Proceedings of the National Academy of Sciences, 121, e2411212121, doi:10.1073/pnas.2411212121, 2024.

Milkov, A. V., Schwietzke, S., Allen, G., Sherwood, O. A., and Etiope, G.: Using global isotopic data to constrain the role of shale gas production in recent increases in atmospheric methane, Scientific Reports, 10, 4199, 2020.

Montzka, S. A., Dlugokencky, E. J., and Butler, J. H.: Non-CO_2 greenhouse gases and climate change, Nature, 476, 43-50, 2011.

Moreira, M., Sternberg, L., Martinelli, L., Victoria, R., Barbosa, E., Bonates, L., and Nepstad, D.: Contribution of transpiration to forest ambient vapour based on isotopic measurements, Global Change Biology, 3, 439-450, 1997.

National data: https://tjj.sc.gov.cn/scstjj/c111701/common_list.shtml, last access: 12 June 2025.

Global Monitoring Laboratory: https://gml.noaa.gov/dv/data/, last access: 12 June 2025.

HYSPLIT Trajectory Model: https://www.ready.noaa.gov/hypub-bin/trajasrc.pl, last access: 12 June 2025.

Nisbet, E. G., Manning, M. R., Lowry, D., Fisher, R. E., Lan, X., Michel, S. E., France, J. L., Nisbet, R. E. R., Bakkaloglu, S., Leitner, S. M., Brooke, C., Röckmann, T., Allen, G., Denier van der Gon, H. A. C., Merbold, L., Scheutz, C., Woolley Maisch, C., Nisbet-Jones, P. B. R., Alshalan, A., Fernandez, J. M., and Dlugokencky, E. J.: Practical paths towards quantifying and mitigating agricultural methane emissions, Proceedings of the Royal Society A: Mathematical, Physical and Engineering Sciences, 481, 20240390, doi:10.1098/rspa.2024.0390, 2025.

Omara, M., Sullivan, M. R., Li, X., Subramanian, R., Robinson, A. L., and Presto, A. A.: Methane emissions from conventional and unconventional natural gas production sites in the Marcellus Shale Basin, Environmental science & technology, 50, 2099-2107, 2016.

Pataki, D. E., Ehleringer, J. R., Flanagan, L. B., Yakir, D., Bowling, D. R., Still, C. J., Buchmann, N., Kaplan, J. O., and Berry, J. A.: The application and interpretation of Keeling plots in terrestrial carbon cycle research, Global Biogeochemical Cycles, 17, 2003.

Peng, L., Ti, C., Yin, B., Dong, W., Li, M., Tao, L., and Yan, X.: Traceability of atmospheric ammonia in a suburban area of the Beijing-Tianjin-Hebei region, Science of The Total Environment, 907, 167935, 2024.

Pereira, A. P. M. F., Rodrigues, L. A. d. C., Santos, E. A. d., Cardoso, T. A. d. O., and Cohen, S. C.: CBRN events management and the use of the Hysplit model: an integrative literature review, Saúde em Debate, 43, 925-938, 2019.

Rella, C. W., Hoffnagle, J., He, Y., and Tajima, S.: Local- and regional-scale measurements of CH_4, $\delta^{13}CH_4$, and C_2H_6 in the Uintah Basin using a mobile stable isotope analyzer, Atmos. Meas. Tech., 8, 4539-4559, 2015.

Rice, A. L., Butenhoff, C. L., Teama, D. G., Röger, F. H., Khalil, M. A. K., and Rasmussen, R. A.: Atmospheric methane isotopic record favors fossil sources flat in 1980s and 1990s with recent increase, Proceedings of the National Academy of Sciences, 113, 10791-10796, 2016.

Saunois, M., Martinez, A., Poulter, B., Zhang, Z., Raymond, P., Regnier, P., Canadell, J. G., Jackson, R. B., Patra, P. K., Bousquet, P., Ciais, P., Dlugokencky, E. J., Lan, X., Allen, G. H., Bastviken, D., Beerling, D. J., Belikov, D. A., Blake, D. R., Castaldi, S., Crippa, M., Deemer, B. R., Dennison, F., Etiope, G., Gedney, N., Höglund-Isaksson, L., Holgerson, M. A., Hopcroft, P. O., Hugelius, G., Ito, A., Jain, A. K., Janardanan, R., Johnson, M. S., Kleinen, T., Krummel, P., Lauerwald, R., Li, T., Liu, X., McDonald, K. C., Melton, J. R., Mühle, J., Müller, J., Murguia-Flores, F., Niwa, Y., Noce, S., Pan, S., Parker, R. J., Peng, C., Ramonet, M., Riley, W. J., Rocher-Ros, G., Rosentreter, J. A., Sasakawa, M., Segers, A., Smith, S. J., Stanley, E. H., Thanwerdas, J., Tian, H., Tsuruta, A., Tubiello, F. N., Weber, T. S., van der Werf, G., Worthy, D. E., Xi, Y., Yoshida, Y., Zhang, W., Zheng, B., Zhu, Q., Zhu, Q., and Zhuang, Q.: Global Methane Budget 2000-2020, Earth Syst. Sci. Data Discuss., 2024, 1-147, 10.5194/essd-2024-115, 2024.

Schoell, M.: The hydrogen and carbon isotopic composition of methane from natural gases of various origins, Geochimica et Cosmochimica Acta, 44, 649-661, 1980.

Schwietzke, S., Sherwood, O. A., Bruhwiler, L. M. P., Miller, J. B., Etiope, G., Dlugokencky, E. J.,

Michel, S. E., Arling, V. A., Vaughn, B. H., White, J. W. C., and Tans, P. P.: Upward revision of global fossil fuel methane emissions based on isotope database, Nature, 538, 88-91, 2016.

Shan, W., Yin, Y., Lu, H., and Liang, S.: A meteorological analysis of ozone episodes using HYSPLIT model and surface data, Atmospheric Research, 93, 767-776, 2009.

Shaw, J. T., Shah, A., Yong, H., and Allen, G.: Methods for quantifying methane emissions using unmanned aerial vehicles: A review, Philosophical Transactions of the Royal Society A, 379, 20200450, 2021.

Sherwood Lollar, B., Westgate, T., Ward, J., Slater, G., and Lacrampe-Couloume, G.: Abiogenic formation of alkanes in the Earth's crust as a minor source for global hydrocarbon reservoirs, Nature, 416, 522-524, 2002.

2023 the statistical bulletin of national economic and social development of Sichuan province: https://tjj.sc.gov.cn/scstjj/c111701/common_list.shtml, last access: 12 June 2025.

Skeie, R. B., Hodnebrog, Ø., and Myhre, G.: Trends in atmospheric methane concentrations since 1990 were driven and modified by anthropogenic emissions, Communications Earth & Environment, 4, 317, 2023.

Stein, A. F., Draxler, R. R., Rolph, G. D., Stunder, B. J. B., Cohen, M. D., and Ngan, F.: NOAA's HYSPLIT Atmospheric Transport and Dispersion Modeling System, Bulletin of the American Meteorological Society, 96, 2059-2077, 2015.

Sun, S., Ma, L., and Li, Z.: A Source-Level Estimation and Uncertainty Analysis of Methane Emission in China's Oil and Natural Gas Sector, 2022.

Suzuki, Y.: Achieving food authenticity and traceability using an analytical method focusing on stable isotope analysis, Analytical Sciences, 37, 189-199, 2021.

Thom, M., Bösinger, R., Schmidt, M., and Levin, I.: The regional budget of atmospheric methane of a highly populated area, Chemosphere, 26, 143-160, 1993.

Tian, H., Lu, C., Ciais, P., Michalak, A. M., Canadell, J. G., Saikawa, E., Huntzinger, D. N., Gurney, K. R., Sitch, S., Zhang, B., Yang, J., Bousquet, P., Bruhwiler, L., Chen, G., Dlugokencky, E., Friedlingstein, P., Melillo, J., Pan, S., Poulter, B., Prinn, R., Saunois, M., Schwalm, C. R., and Wofsy, S. C.: The terrestrial biosphere as a net source of greenhouse gases to the atmosphere, Nature, 531, 225-228, 2016.

Tibrewal, K., Ciais, P., Saunois, M., Martinez, A., Lin, X., Thanwerdas, J., Deng, Z., Chevallier, F., Giron, C., and Albergel, C.: Assessment of methane emissions from oil, gas and coal sectors across inventories and atmospheric inversions, Communications Earth & Environment, 5, 26, 2024.

Townsend-Small, A., Ferrara, T. W., Lyon, D. R., Fries, A. E., and Lamb, B. K.: Emissions of coalbed and natural gas methane from abandoned oil and gas wells in the United States, Geophysical Research Letters, 43, 2283-2290, 2016.

Tyler, S. C.: Stable carbon isotope ratios in atmospheric methane and some of its sources, Journal of Geophysical Research: Atmospheres, 91, 13232-13238, 1986.

Summary Report: Global Anthropogenic Non-CO2 Greenhouse Gas Emissions: 1990–2030: https://nepis.epa.gov/Exe/ZyPDF.cgi/P100FE8H.PDF?Dockey=P100FE8H.PDF, last access: 12 June 2025.

Wang, Y., Chen, J., Pang, X., Zhang, B., Chen, Z., Zhang, G., Luo, G., and He, L.: Origin of deep sour natural gas in the Ordovician carbonate reservoir of the Tazhong Uplift, Tarim Basin, northwest China: Insights from gas geochemistry and formation water, Marine and Petroleum

Geology, 91, 532-549, 2018.

Zazzeri, G., Lowry, D., Fisher, R. E., France, J. L., Lanoisellé, M., and Nisbet, E. G.: Plume mapping and isotopic characterisation of anthropogenic methane sources, Atmospheric Environment, 110, 151-162, 2015.

Zhang, B., Chen, G. Q., Li, J. S., and Tao, L.: Methane emissions of energy activities in China 1980–2007, Renewable and Sustainable Energy Reviews, 29, 11-21, 2014.

Zhang, S. and Zhu, G.: Natural gas origins of large and medium-scale gas fields in China sedimentary basins, Science in China Series D: Earth Sciences, 51, 1-13, 2008.

Zhang, S., He, K., Hu, G., Mi, J., Ma, Q., Liu, K., and Tang, Y.: Unique chemical and isotopic characteristics and origins of natural gases in the Paleozoic marine formations in the Sichuan Basin, SW China: Isotope fractionation of deep and high mature carbonate reservoir gases, Marine and Petroleum Geology, 89, 68-82, 2018.

Zhao, Y., Zheng, B., Saunois, M., Ciais, P., Hegglin, M. I., Lu, S., Li, Y., and Bousquet, P.: Air pollution modulates trends and variability of the global methane budget, Nature, 10.1038/s41586-025-09004-z, 2025.

Zhu, G., Wang, Z., Dai, J., and Su, J.: Natural gas constituent and carbon isotopic composition in petroliferous basins, China, Journal of Asian Earth Sciences, 80, 1-17, 2014.

Zou, Y.-R., Cai, Y., Zhang, C., Zhang, X., and Peng, P. a.: Variations of natural gas carbon isotope-type curves and their interpretation – A case study, Organic Geochemistry, 38, 1398-1415, 2007.